Measurement of Polarization Observables in Double-pion Photoproduction from the FROST Experiment at Jefferson Lab

Priyashree Roy

Florida State University, Tallahassee, Florida

Prospectus Defense

08/20/2013

Outline

The Strong Interaction

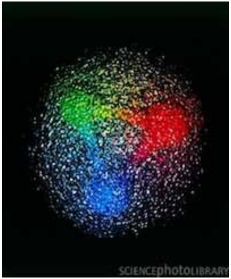

Hadrons (baryons and mesons) consist of valence quarks, sea quarks and gluons - not a simple picture !

The Strong Interaction

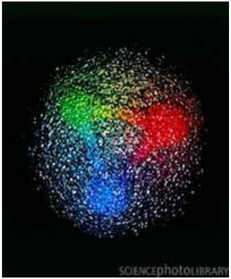

Hadrons (baryons and mesons) consist of valence quarks, sea quarks and gluons - not a simple picture !

How do quarks and gluons interact ? QCD - the theory of the strong force to describe quark-gluon interaction in hadrons.

- Consider a quark-antiquark pair.

The Strong Interaction

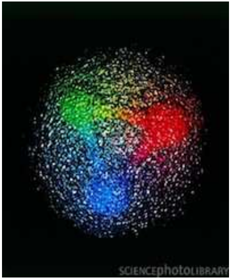

Hadrons (baryons and mesons) consist of valence quarks, sea quarks and gluons - not a simple picture !

How do quarks and gluons interact ? QCD - the theory of the strong force to describe quark-gluon interaction in hadrons.

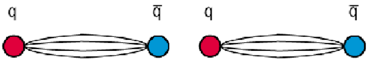

- We can't isolate the quarks .. **Color confinement.**
- Why confinement? No analytic proof that QCD should be confining.

Understanding Baryon Structure

How many degrees of freedom do baryons have? Understanding non-perturbative aspects of the baryon structure -

- Lattice QCD calculations need a lot of improvement in computational analysis.
- Baryon Spectroscopy - understanding the interactions and dynamics of the constituents of the baryons.

  Constituent Quark Model for baryons - 3 "constituent quarks" placed in a linearly confining potential.

Understanding Baryon Structure

How many degrees of freedom do baryons have? Understanding non-perturbative aspects of the baryon structure -

- Lattice QCD calculations need a lot of improvement in computational analysis.
- Baryon Spectroscopy - understanding the interactions and dynamics of the constituents of the baryons.

  Constituent Quark Model for baryons - 3 "constituent quarks" placed in a linearly confining potential.

Understanding Baryon Structure

How many degrees of freedom do baryons have? Understanding non-perturbative aspects of the baryon structure -

- Lattice QCD calculations need a lot of improvement in computational analysis.
- Baryon Spectroscopy - understanding the interactions and dynamics of the constituents of the baryons.

  Constituent Quark Model for baryons - 3 "constituent quarks" placed in a linearly confining potential.

CQM Predictions for Baryons

Predictions for isospin $1/2$ strangeness zero baryons.
U. Löring *(et al.) Eur.Phys.J.A* **10**,*395 (2001)*

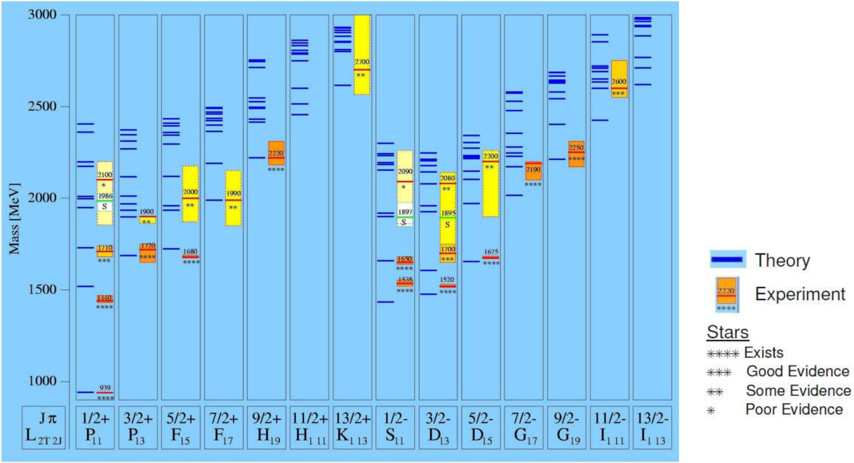

Baryon spectroscopy

Many undetected resonances, specially for W > 1.7 GeV. Possible reasons -

- The model may not be completely applicable.
- Missing resonances don't couple to π N. Electroproduction and photoproduction experiments could reveal them.
- Baryon resonances are broad and close together.

Baryon spectroscopy

Many undetected resonances, specially for W > 1.7 GeV. Possible reasons -

- The model may not be completely applicable.
- Missing resonances don't couple to π N. Electroproduction and photoproduction experiments could reveal them.
- Baryon resonances are broad and close together.

Baryon spectroscopy

Many undetected resonances, specially for W > 1.7 GeV. Possible reasons -

- The model may not be completely applicable.
- Missing resonances don't couple to π N. Electroproduction and photoproduction experiments could reveal them.
- Baryon resonances are broad and close together.

Baryon spectroscopy

Many undetected resonances, specially for W > 1.7 GeV. Possible reasons -

- The model may not be completely applicable.
- Missing resonances don't couple to π N. Electroproduction and photoproduction experiments could reveal them.
- Baryon resonances are broad and close together.

Baryon spectroscopy

Many undetected resonances, specially for W > 1.7 GeV. Possible reasons -

- The model may not be completely applicable.
- Missing resonances don't couple to π N. Electroproduction and photoproduction experiments could reveal them.
- Baryon resonances are broad and close together.

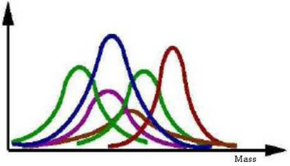

Baryon spectroscopy

Many undetected resonances, specially for W > 1.7 GeV. Possible reasons -

- The model may not be completely applicable.
- Missing resonances don't couple to π N. Electroproduction and photoproduction experiments could reveal them.
- Baryon resonances are broad and close together. Need sophisticated tools to separate them -
  - Spin observables, cross sections.
  - Partial Wave Analysis.

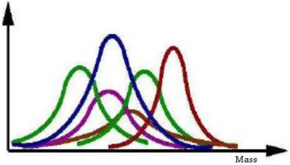

Baryon spectroscopy

Many undetected resonances, specially for W > 1.7 GeV. Possible reasons -

- The model may not be completely applicable.
- Missing resonances don't couple to π N. Electroproduction and photoproduction experiments could reveal them.
- Baryon resonances are broad and close together. Need sophisticated tools to separate them -
  - Spin observables, cross sections.
  - Partial Wave Analysis.

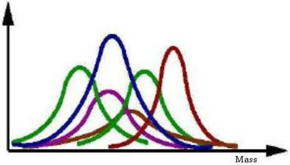

Baryon spectroscopy

Many undetected resonances, specially for W > 1.7 GeV. Possible reasons -

- The model may not be completely applicable.
- Missing resonances don't couple to π N. Electroproduction and photoproduction experiments could reveal them.
- Baryon resonances are broad and close together. Need sophisticated tools to separate them -
  - ◇ Spin observables, cross sections.
  - ◇ Partial Wave Analysis.

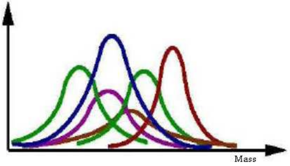

Baryon spectroscopy

Many undetected resonances, specially for W > 1.7 GeV. Possible reasons -

- The model may not be completely applicable.
- Missing resonances don't couple to π N. Electroproduction and photoproduction experiments could reveal them.
- Baryon resonances are broad and close together. Need sophisticated tools to separate them -
  - ◇ Spin observables, cross sections.
  - ◇ Partial Wave Analysis.

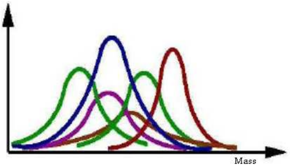

Baryon spectroscopy

Many undetected resonances, specially for W > 1.7 GeV. Possible reasons -

- The model may not be completely applicable.
- Missing resonances don't couple to π N. Electroproduction and photoproduction experiments could reveal them.
- Baryon resonances are broad and close together. Need sophisticated tools to separate them -
  - ◇ Spin observables, cross sections.
  - ◇ Partial Wave Analysis.

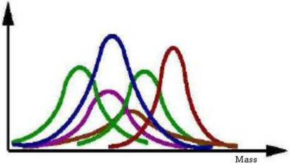

Light flavored baryon spectroscopy- JLab (U.S.),CBELSA/TAPS at Universität Bonn (Germany), Mainz Microtron (Germany), LEPS (Japan)...

Motivation

Reaction of interest : $\vec{\gamma}\vec{p} \to p\pi^+\pi^-$.
(1.6 $<$ W $<$ 2.1 GeV).

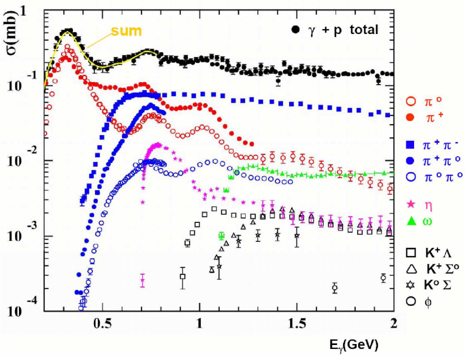

Extract polarization observables for linearly polarized beam and transversely polarized target from FROST experiment at JLab.

Motivation

Reaction of interest : $\vec{\gamma}\vec{p} \rightarrow p\pi^+\pi^-$.
(1.6 $<$ W $<$ 2.1 GeV).

Advantages ->

- biggest contributor to the cross section for W $>$ 1.7 GeV.
- higher mass resonances likely to undergo sequential decay.
  E.g., $\gamma p \rightarrow N^* \rightarrow \Delta\pi \rightarrow p\pi^+\pi^-$
  $\gamma p \rightarrow N^* \rightarrow p\rho \rightarrow p\pi^+\pi^-$

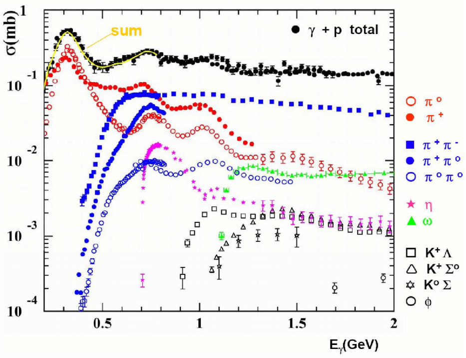

Extract polarization observables for linearly polarized beam and transversely polarized target from FROST at JLab.

Motivation

Reaction of interest : $\vec{\gamma}\vec{p} \rightarrow p\pi^{+}\pi^{-}$.
(1.6 $<$ W $<$ 2.1 GeV).

Advantages ->

- biggest contributor to the cross section for W $>$ 1.7 GeV.
- higher mass resonances likely to undergo sequential decay.
  E.g., $\gamma p \rightarrow N^{*} \rightarrow \Delta\pi \rightarrow p\pi^{+}\pi^{-}$
  $\gamma p \rightarrow N^{*} \rightarrow p\rho \rightarrow p\pi^{+}\pi^{-}$

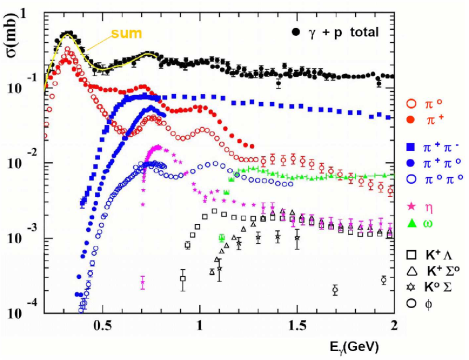

Extract polarization observables for linearly polarized beam and transversely polarized target from FROST at JLab.

Motivation

Reaction of interest : $\vec{\gamma}\vec{p} \rightarrow p\pi^+\pi^-$.
(1.6 $<$ W $<$ 2.1 GeV).

Advantages ->

- biggest contributor to the cross section for W $>$ 1.7 GeV.
- higher mass resonances likely to undergo sequential decay.
  E.g., $\gamma p \rightarrow N^* \rightarrow \Delta\pi \rightarrow p\pi^+\pi^-$
  $\gamma p \rightarrow N^* \rightarrow p\rho \rightarrow p\pi^+\pi^-$

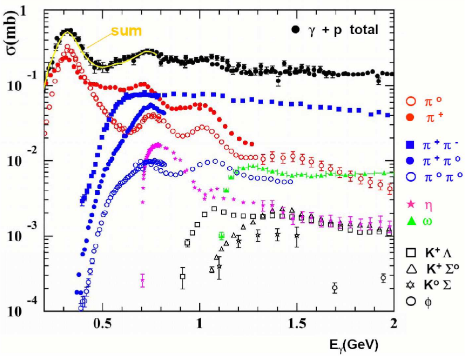

Extract polarization observables for linearly polarized beam and transversely polarized target from FROST at JLab.

Polarization observables

For $p\pi\pi$ state, w/o measuring polarization of recoiling p, reaction rate I -

$$I = I_0\{(1 + \bar{\Lambda}_i \cdot \bar{P})$$
$$+\delta_{\odot}(I^{\odot} + \bar{\Lambda}_i \cdot \bar{P}^{\odot})$$
$$+\delta_l[sin2\beta(I^s + \bar{\Lambda}_i \cdot \bar{P}^s)cos2\beta(I^c + \bar{\Lambda}_i \cdot \bar{P}^c)]\}$$

15 polarization observables

- $I^{\odot}$ - published results for 1.35<W<2.30 GeV [1] and for 0.57<W<0.81 GeV [2].

  [1] S.Strauch *et al. Phys. Rev. Lett.* ***95****, 162003 (2005).*

  [2] D. Krambrich *et al. Phys. Rev. Lett.* ***103****, 052002 (2009).*

- $P_z^{\odot}$ - results on helicity dependent cross section difference.

  J. Ahrens *et al. Eur. Phys. J.* ***A34****, 11 (2007).*

- Preliminary results from FROST expt for $I^{s,c}$, $I^{\odot}$, $P_z^{\odot}$, P_z, $P_z^{s,c}$ using polarized beam & unpolarized/longitudinally polarized target.

Polarization observables

For $p\pi\pi$ state, w/o measuring polarization of recoiling p, reaction rate I -

$$I = I_0\{(1 + \bar{\Lambda}_i \cdot \bar{P})$$
$$+\delta_\odot(I^\odot + \bar{\Lambda}_i \cdot \bar{P}^\odot)$$
$$+\delta_l[sin2\beta(I^s + \bar{\Lambda}_i \cdot \bar{P}^s)cos2\beta(I^c + \bar{\Lambda}_i \cdot \bar{P}^c)]\}$$

15 polarization observables

- $I^\odot$ - published results for 1.35<W<2.30 GeV [1] and for 0.57<W<0.81 GeV [2].

  [1] S.Strauch *et al. Phys. Rev. Lett.* ***95****, 162003 (2005).*

  [2] D. Krambrich *et al. Phys. Rev. Lett.* ***103****, 052002 (2009).*

- $P_z^\odot$ - results on helicity dependent cross section difference.

  J. Ahrens *et al. Eur. Phys. J.* ***A34****, 11 (2007).*

- Preliminary results from FROST expt for $I^{s,c}$, $I^\odot$, $P_z^\odot$, P_z, $P_z^{s,c}$ using polarized beam & unpolarized/longitudinally polarized target.

Polarization observables

For $p\pi\pi$ state, w/o measuring polarization of recoiling p, reaction rate I -

$$I = I_0\{(1 + \bar{\Lambda}_i \cdot \bar{P})$$
$$+\delta_{\odot}(I^{\odot} + \bar{\Lambda}_i \cdot \bar{P}^{\odot})$$
$$+\delta_l[sin2\beta(I^s + \bar{\Lambda}_i \cdot \bar{P}^s)cos2\beta(I^c + \bar{\Lambda}_i \cdot \bar{P}^c)]\}$$

15 polarization observables

- $I^{\odot}$ - published results for 1.35<W<2.30 GeV [1] and for 0.57<W<0.81 GeV [2].

  [1] S.Strauch *et al. Phys. Rev. Lett.* ***95****, 162003 (2005).*

  [2] D. Krambrich *et al. Phys. Rev. Lett.* ***103****, 052002 (2009).*

- $P_z^{\odot}$ - results on helicity dependent cross section difference.

  J. Ahrens *et al. Eur. Phys. J.* ***A34****, 11 (2007).*

- Preliminary results from FROST expt for $I^{s,c}$, $I^{\odot}$, $P_z^{\odot}$, P_z, $P_z^{s,c}$ using polarized beam & unpolarized/longitudinally polarized target.

Polarization observables

For $p\pi\pi$ state, w/o measuring polarization of recoiling p, reaction rate I -

$$I = I_0\{(1 + \bar{\Lambda}_i \cdot \bar{P}) + \delta_\odot(I^\odot + \bar{\Lambda}_i \cdot \bar{P}^\odot) + \delta_l[sin2\beta(I^s + \bar{\Lambda}_i \cdot \bar{P}^s)cos2\beta(I^c + \bar{\Lambda}_i \cdot \bar{P}^c)]\}$$

15 polarization observables

- $I^\odot$ - published results for 1.35<W<2.30 GeV [1] and for 0.57<W<0.81 GeV [2].

  [1] S.Strauch *et al. Phys. Rev. Lett.* ***95**, 162003 (2005).*

  [2] D. Krambrich *et al. Phys. Rev. Lett.* ***103**, 052002 (2009).*

- $P_z^\odot$ - results on helicity dependent cross section difference.

  J. Ahrens *et al. Eur. Phys. J.* ***A34**, 11 (2007).*

- Preliminary results from FROST expt for $I^{s,c}$, $I^\odot$, $P_z^\odot$, P_z, $P_z^{s,c}$ using polarized beam & unpolarized/longitudinally polarized target.

Polarization observables

In my analysis -
linearly polarized beam -> $\delta_{\odot} = 0$
transversely polarized target -> $\Lambda_z = 0$

$$I = I_0\{(1 + \Lambda_x \; P_x + \Lambda_y \; P_y) + \delta_l [sin(2\beta)(\; I^s + \Lambda_x \; P_x^s + \Lambda_y \; P_y^s \;) \; cos(2\beta)(\; I^c \; + \Lambda_x \; P_x^c \; + \Lambda_y \; P_y^c \;)]\}$$

8 Polarization Observables - 6 first time measurements !

Extracting polarization observables for 1.6$<$W$<$2.1 GeV in this thesis -> bring us closer to a "complete set" to get unambigious solutions to the scattering amplitudes.

Outline

The FROST experiment in Jefferson Lab, VA

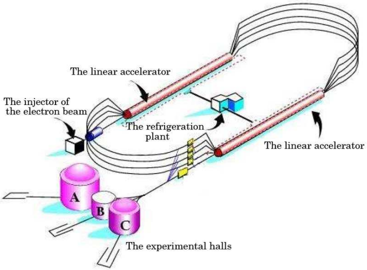

- "g9b" experiment in Hall B (Mar - Aug 2010)
- **FROST** - "Frozen Spin Target"
- e^- beam energy upto 5.6 GeV.

The FROST experiment in Jefferson Lab, VA

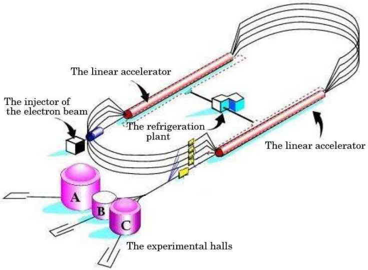

- "g9b" experiment in Hall B (Mar - Aug 2010)
- **FROST** - "Frozen Spin Target"
- e^- beam energy upto 5.6 GeV.

The FROST experiment in Jefferson Lab, VA

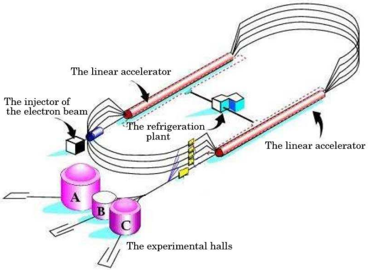

- "g9b" experiment in Hall B (Mar - Aug 2010)
- **FROST** - "Frozen Spin Target"
- e^- beam energy upto 5.6 GeV.

The FROST experiment in Jefferson Lab, VA

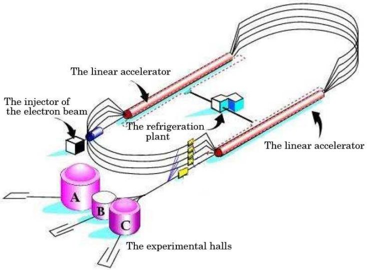

- "g9b" experiment in Hall B (Mar - Aug 2010)
- **FROST** - "Frozen Spin Target"
- e^- beam energy upto 5.6 GeV.

Layout of the g9b experimental setup

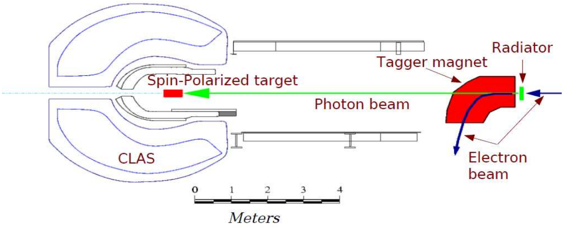

- Linearly polarized photon beam by Bremsstrahlung radiation at the diamond radiator.

Layout of the g9b experimental setup

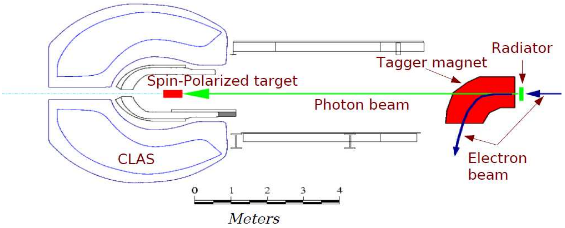

- Linearly polarized photon beam by Bremsstrahlung radiation at the diamond radiator.

Layout of the g9b experimental setup

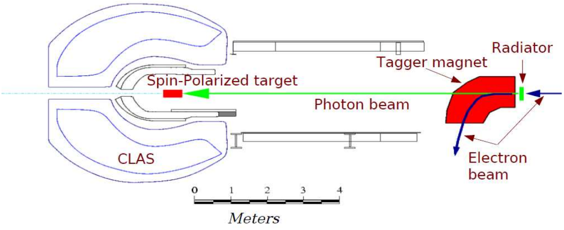

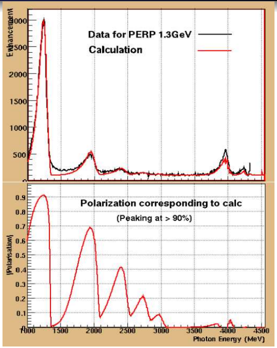

- Linearly polarized photon beam by Bremsstrahlung radiation at the diamond radiator.
- Coherent edge - 0.9 to 2.1 GeV in steps of 200 MeV.
- FRozen Spin Target : TEMPO doped butanol C_4H_9OH.
- CLAS detector to detect charged particles.

Layout of the g9b experimental setup

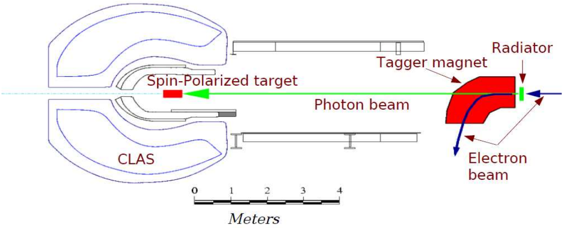

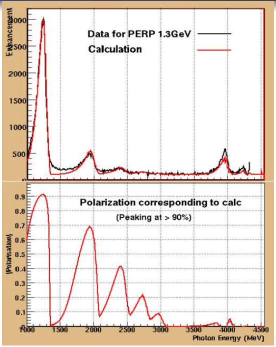

- Linearly polarized photon beam by Bremsstrahlung radiation at the diamond radiator.
- Coherent edge - 0.9 to 2.1 GeV in steps of 200 MeV.
- FRozen Spin Target : TEMPO doped butanol C_4H_9OH.
- CLAS detector to detect charged particles.

Layout of the g9b experimental setup

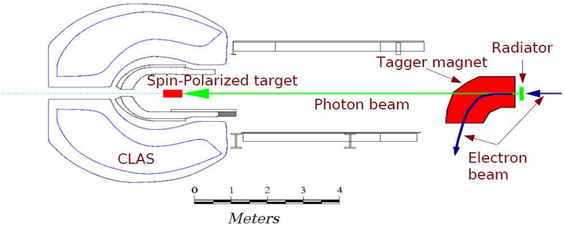

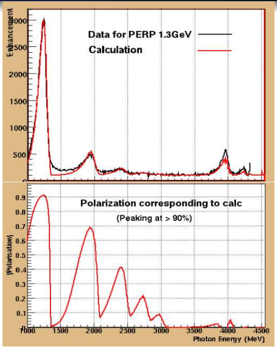

- Linearly polarized photon beam by Bremsstrahlung radiation at the diamond radiator.
- Coherent edge - 0.9 to 2.1 GeV in steps of 200 MeV.
- FRozen Spin Target : TEMPO doped butanol C_4H_9OH.
- CLAS detector to detect charged particles.

FROzen Spin Target

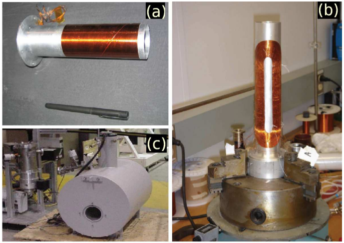

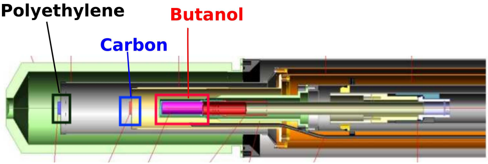

- (c) Polarizing field 5T. DNP technique.
- (a),(b) holding magnets.
- Low T (30 mK) and high B (5 T) for long relaxation time (3400 hrs w/ beam and 4000 hrs w/o beam).
- Av. deg. of polarization - 84 to 86 %.

FROzen Spin Target

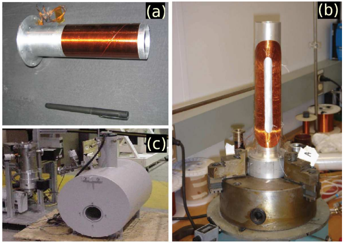

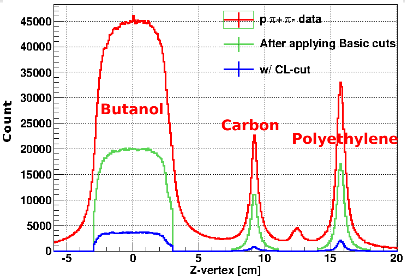

- (c) Polarizing field 5T. DNP technique.
- (a),(b) holding magnets.
- Low T (30 mK) and high B (5 T) for long relaxation time (3400 hrs w/ beam and 4000 hrs w/o beam).
- Av. deg. of polarization - 84 to 86 %.

The CLAS detector

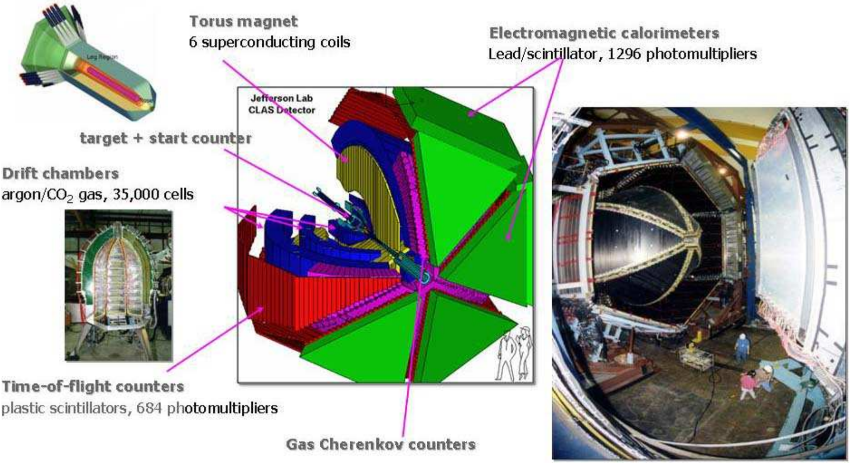

Outline

The topology cut

Topologies originating from the $p\pi^+\pi^-$ final state -

- Top 1 : $\gamma\ p \rightarrow p\ \ \pi^+(\pi^-)$
- Top 2 : $\gamma\ p \rightarrow p\ \ \pi^-(\pi^+)$
- Top 3 : $\gamma\ p \rightarrow \pi^+\pi^-\ \ (p)$ (not considered as it could be a missing neutron)
- Top 4 : $\gamma\ p \rightarrow p\ \ \pi^+\pi^-$
- Particle id from v and p information from Drift Chambers, Start Counter and Time of Flight.

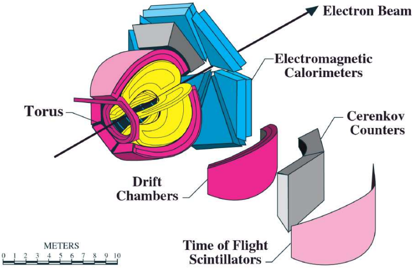

The beta cut

- The beta cut :- $\Delta\beta < 3\sigma$
- $\Delta\beta = \beta_1 - \beta_2,\ \beta_1 = \frac{v}{c},\ \beta_2 = \frac{p}{\sqrt{p^2+m^2}}$

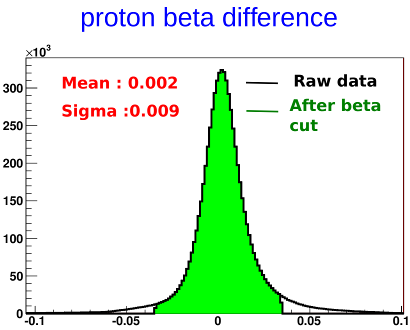

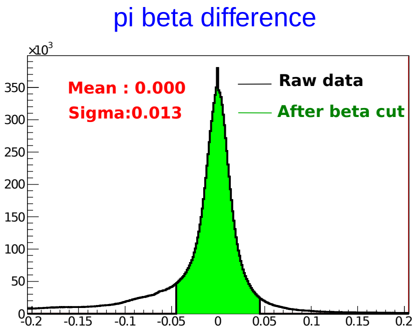

The beta cut

- Beta cut : identifying pions and protons
- $\Delta\beta = \beta_1 - \beta_2,\ \beta_1 = \frac{v}{c},\ \beta_2 = \frac{p}{\sqrt{p^2+m^2}}$

Before beta cut

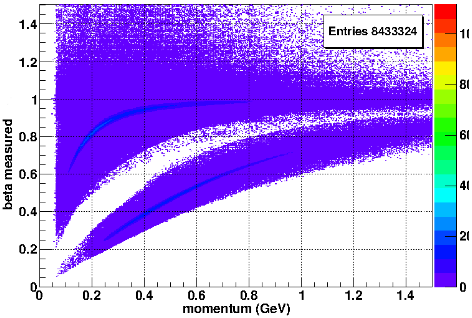

After beta cut

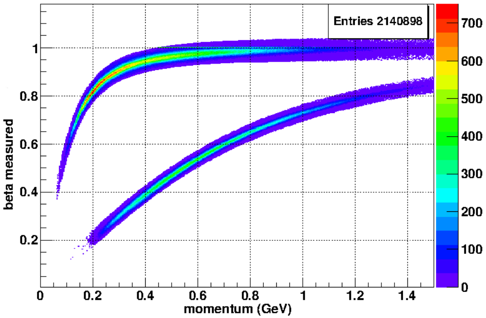

Photon selection

2 ns photon bunches.

Many candidate photons per event. Δt = t(event vertex time) - t(candidate photon at the vertex).

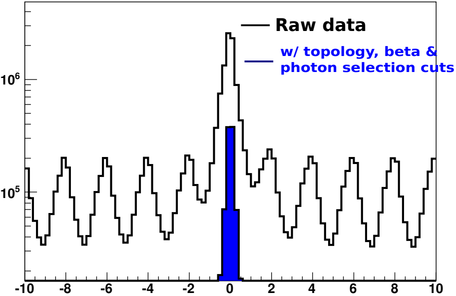

- Photon selection cuts-
  - 1 photon for each final state particle.
  - All final state particles originated from the same incident photon.
- $|\Delta t| < 0.5$ ns after applying the photon selection cuts.

Photon selection

2 ns photon bunches.

Many candidate photons per event. $\Delta t = $ t(event vertex time) - t(candidate photon at the vertex).

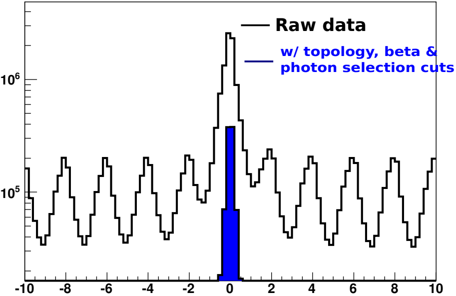

- Photon selection cuts-
  - 1 photon for each final state particle.
  - All final state particles originated from the same incident photon.
- $|\Delta t| < 0.5$ ns after applying the photon selection cuts.

Photon selection

2 ns photon bunches.

Many candidate photons per event. Δt = t(event vertex time) - t(candidate photon at the vertex).

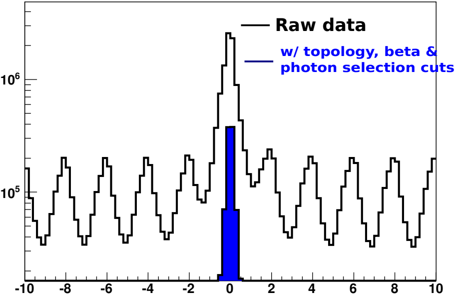

- Photon selection cuts-
  - 1 photon for each final state particle.
  - All final state particles originated from the same incident photon.
- $|\Delta t| < 0.5$ ns after applying the photon selection cuts.

Photon selection

2 ns photon bunches.

Many candidate photons per event. $\Delta t = $ t(event vertex time) - t(candidate photon at the vertex).

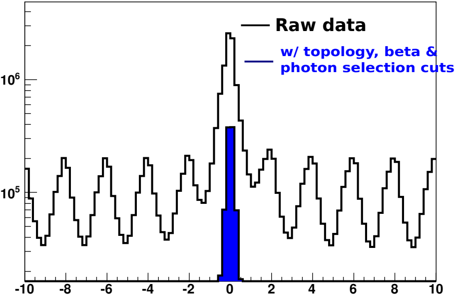

- Photon selection cuts-
  - ◇ 1 photon for each final state particle.
  - ◇ All final state particles originated from the same incident photon.
- $|\Delta t| < 0.5$ ns after applying the photon selection cuts.

Kinematic fitting

- Enforcing energy-momentum conservation in each event.
- Fit quality determined by -
  - Pull distribution - measures how much the fitter had to alter the fit parameter. Good event -> pull mean $\sim$ 0 and pull $\sigma \sim$ 1.
  - Confidence level (CL) distribution - returns value 0 to 1 for each event.

    Good events -> Flat CL distribution.

Kinematic fitting

- Enforcing energy-momentum conservation in each event.
- Fit quality determined by -
  - Pull distribution - measures how much the fitter had to alter the fit parameter. Good event -> pull mean $\sim$ 0 and pull $\sigma \sim$ 1.
  - Confidence level (CL) distribution - returns value 0 to 1 for each event.

    Good events -> Flat CL distribution.

Kinematic fitting

- Enforcing energy-momentum conservation in each event.
- Fit quality determined by -

◇ Pull distribution - measures how much the fitter had to alter the fit parameter. Good event -> pull mean $\sim$ 0 and pull $\sigma \sim$ 1.

◇ Confidence level (CL) distribution - returns value 0 to 1 for each event.

Good events -> Flat CL distribution.

Kinematic fitting

- Enforcing energy-momentum conservation in each event.

- Fit quality determined by -

◇ Pull distribution - measures how much the fitter had to alter the fit parameter. Good event -> pull mean $\sim$ 0 and pull $\sigma \sim$ 1.

◇ Confidence level (CL) distribution - returns value 0 to 1 for each event.

Good events -> Flat CL distribution.

Kinematic fitting

- Enforcing energy-momentum conservation in each event.
- Fit quality determined by -

◇ Pull distribution - measures how much the fitter had to alter the fit parameter. Good event -> pull mean $\sim$ 0 and pull $\sigma \sim$ 1.

◇ Confidence level (CL) distribution - returns value 0 to 1 for each event.

Good events -> Flat CL distribution.

Energy and momentum correction

- Eloss correction for energy lost by the particles while traveling to the drift chambers.
- Momentum correction for the final state particles using the pull distributions.
- Photon energy correction needed mainly because of Tagger sagging.

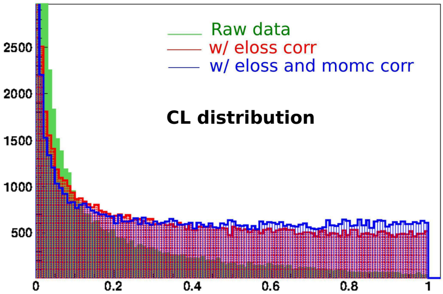

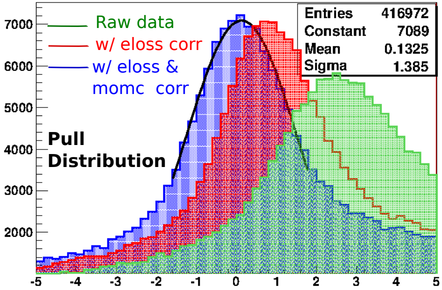

Confidence level and Pull distributions

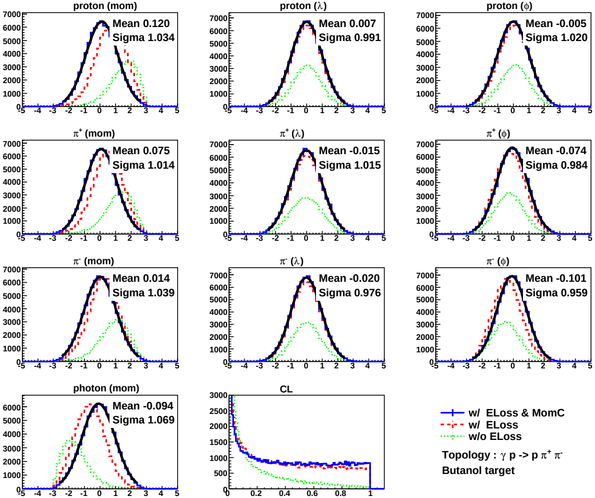

- Select events above 5 % confidence level -

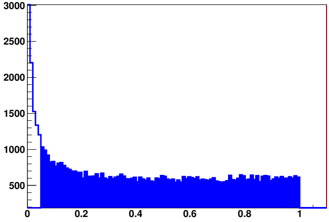

Missing Mass Example

Pion invariant mass $= 139.6$ MeV.

$\gamma \quad p -> p \quad \pi^{+}$ (Missing $\quad \pi^{-}$)

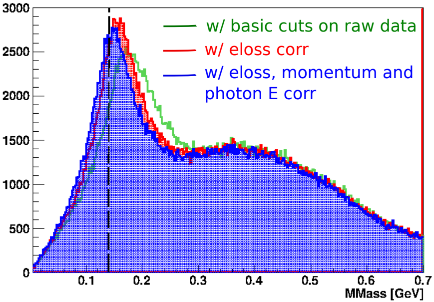

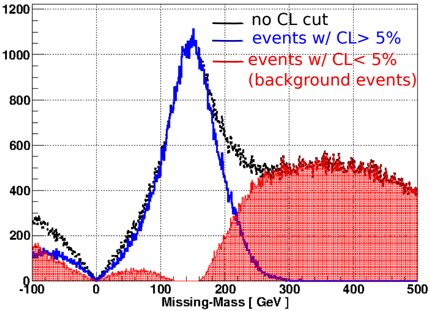

- KFit doesn't distinguish between events originating from free protons and bound nucleons -> need event based quality factor (probability that the event came from the signal distribution).

Outline

Outlook

- Event selection process has almost been accomplished.
- About 3.5 % ($\sim$ 19 million out of 8.4 billion events) of total no. of events are selected after applying all the cuts.

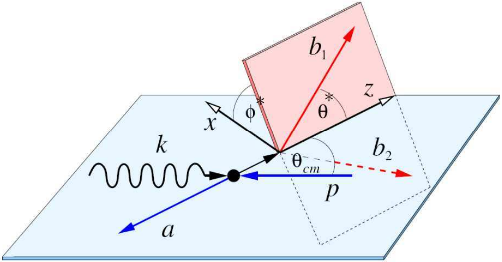

- Production plane (shown in blue) formed by incident photon and recoiling p in the c.o.m. frame.
- 2 pion plane (shown in pink) formed by recoiling p and pions in the 2-pion rest frame.

Outlook

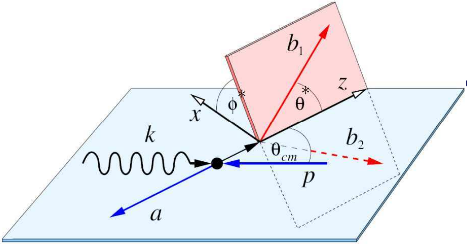

- 5 independent variables needed to describe the kinematics $(E_\gamma, \phi^*, \theta^*, \theta_{c.m.}, m_{p\pi^+})$.
- Event based quality factor will be very useful -
  - in separating signal from background originating from the bound nucleons.
  - in studying asymmetries; no need to find an overall dilution factor each time.

Outlook

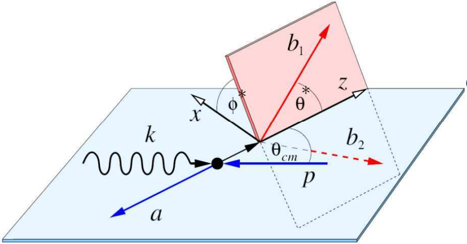

- 5 independent variables needed to describe the kinematics ($E_\gamma, \phi^*, \theta^*, \theta_{c.m.}, m_{p\pi^+}$).
- Event based quality factor will be very useful -
  - in separating signal from background originating from the bound nucleons.
  - in studying asymmetries; no need to find an overall dilution factor each time.

Outlook

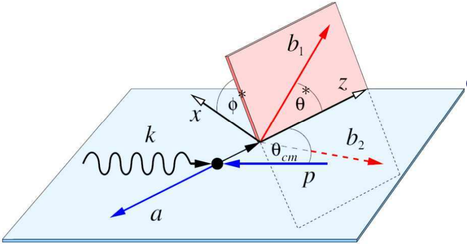

- 5 independent variables needed to describe the kinematics $(E_\gamma, \phi^*, \theta^*, \theta_{c.m.}, m_{p\pi^+})$.
- Event based quality factor will be very useful -
  - in separating signal from background originating from the bound nucleons.
  - in studying asymmetries; no need to find an overall dilution factor each time.

Some examples of polarization observables

For $p\pi\pi$ state, w/o measuring polarization of recoiling p, reaction rate I -

$$I = I_0\{(1 + \bar{\Lambda}_i \cdot \bar{P}) + \delta_{\odot}(I^{\odot} + \bar{\Lambda}_i \cdot \bar{P}^{\odot}) + \delta_l[sin2\beta(I^s + \bar{\Lambda}_i \cdot \bar{P}^s)cos2\beta(I^c + \bar{\Lambda}_i \cdot \bar{P}^c)]\}$$

$I^{\odot}$,$P_z^{\odot}$ and P_z by S. Park, FSU (S. Park, A Dissertation Thesis, Summer Semester, 2013).

Some examples of polarization observables

$$I^{\odot} = \frac{1}{\bar{\delta}_{\odot}(W)} \frac{\{N(\rightarrow;W,\varphi_{\pi^+})_{beam} - N(\leftarrow;W,\varphi_{\pi^+})_{beam}\}}{\{N(\rightarrow;W,\varphi_{\pi^+})_{beam} + N(\leftarrow;W,\varphi_{\pi^+})_{beam}\}}$$

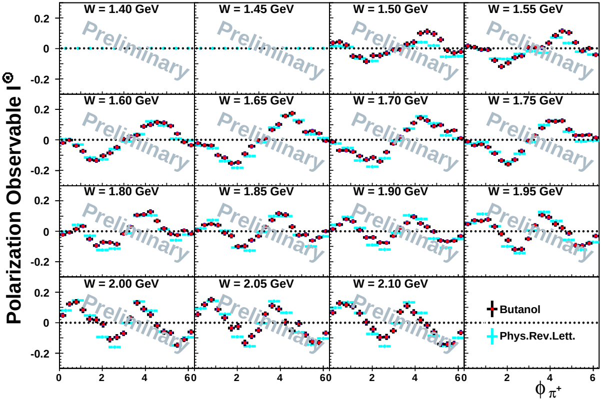

S.Strauch *et al. Phys. Rev. Lett.* ***95****, 162003 (2005).*

Some examples of polarization observables

$$P_z^{\odot} = \frac{1}{\bar{\Lambda}_z(W) \bullet \bar{\delta}_{\odot}} \frac{\{N(W,\varphi_{\pi^+})_{3/2} - N(W,\varphi_{\pi^+})_{1/2}\}}{\{N(W,\varphi_{\pi^+})_{3/2} + N(W,\varphi_{\pi^+})_{1/2}\}}$$

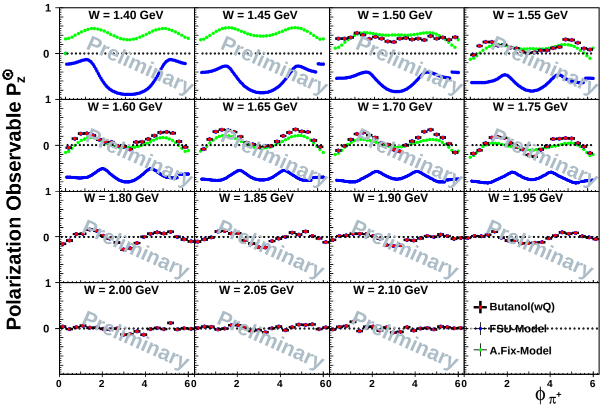

FSU model by Winston Roberts.
A. Fix model (Eur. Phys. J. **A25**, 115-135, 2005.)

Some examples of polarization observables

$$P_z = \frac{1}{\bar{\Lambda}_z(W)} \frac{\{N(\Rightarrow; W, \varphi_{\pi^+})_{target} - N(\Leftarrow; W, \varphi_{\pi^+})_{target}\}}{\{N(\Rightarrow; W, \varphi_{\pi^+})_{target} + N(\Leftarrow; W, \varphi_{\pi^+})_{target}\}}$$

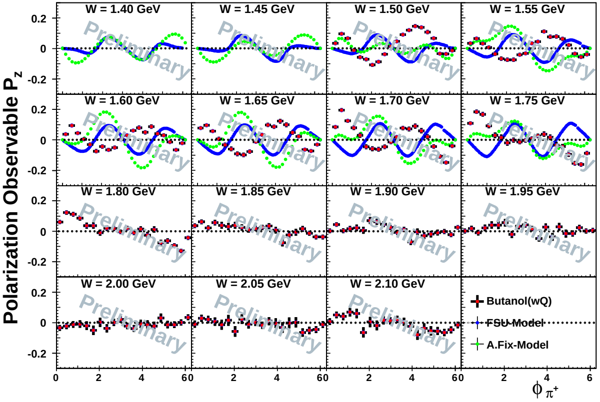

FSU model by Winston Roberts.
A. Fix model (Eur. Phys. J. **A25**, 115-135, 2005.)

Summary

- Reaction of interest: $\vec{\gamma}\vec{p} \rightarrow p\pi^+\pi^-$, linearly polarized photon beam, transversely polarized target.

- Extracting I^s, I^c, $P_{x,y}$, $P^{s,c}_{x,y}$ for 1.6<W<2.1 GeV will bring us closer to a "complete set" to get unambigious solutions to the scattering amplitudes.

- Models based on observables from photoproduction experiments will provide a better understanding of the systematics of the baryon spectrum.

Summary

- Reaction of interest: $\vec{\gamma}\vec{p} \rightarrow p\pi^+\pi^-$, linearly polarized photon beam, transversely polarized target.

- Extracting I^s, I^c, $P_{x,y}$, $P^{s,c}_{x,y}$ for 1.6<W<2.1 GeV will bring us closer to a "complete set" to get unambigious solutions to the scattering amplitudes.

- Models based on observables from photoproduction experiments will provide a better understanding of the systematics of the baryon spectrum.

Summary

- Reaction of interest: $\vec{\gamma}\vec{p} \rightarrow p\pi^+\pi^-$, linearly polarized photon beam, transversely polarized target.

- Extracting I^s, I^c, $P_{x,y}$, $P^{s,c}_{x,y}$ for 1.6<W<2.1 GeV will bring us closer to a "complete set" to get unambigious solutions to the scattering amplitudes.

- Models based on observables from photoproduction experiments will provide a better understanding of the systematics of the baryon spectrum.

HUGS 2013 Summer School at JLab

Thank You!

Tagger

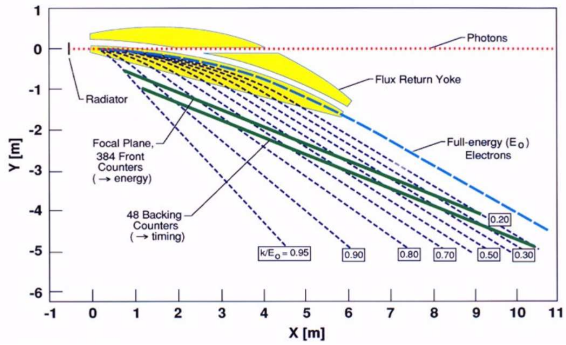
Photons
Flux Return Yoke
Radiator
Focal Plane, 384 Front Counters (→ energy)
48 Backing Counters (→ timing)
Full-energy (E0) Electrons
k/E0 = 0.95
0.90
0.80
0.70
0.50
0.30
0.20
Y [m]
X [m]
1
0
-1
-2
-3
-4
-5
-6
-1
0
1
2
3
4
5
6
7
8
9
10
11

Polarizing the target

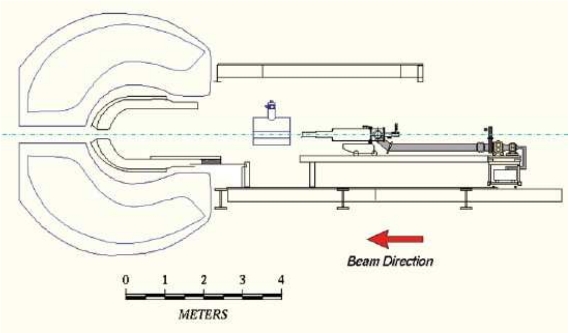

Tagger

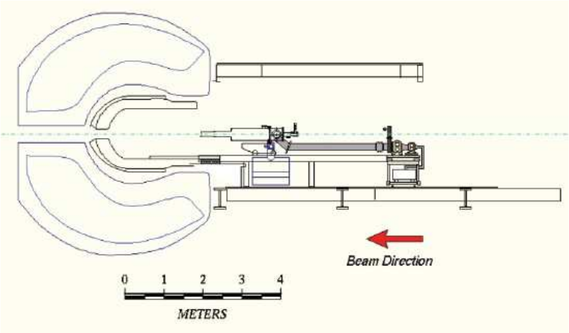

Pull and CL

Pull, $z_i = \frac{\eta_i - y_i}{\sqrt{\sigma^2(\eta_i) - \sigma^2(y_i)}}$

CL $= \int_{\chi^2}^{\infty} f(z;n)dz$, χ^2 is probability function possessing n d.o.f. f is the probability that a χ^2 from the theoretical distribution is greater than the χ^2 from the fit.

Dilution factor

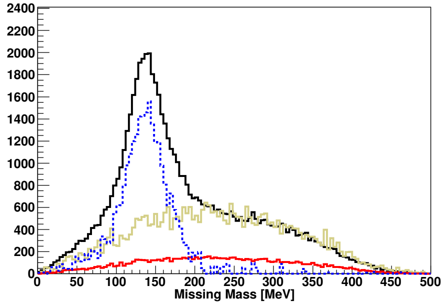

Ideal dilution factor for butanol, $D = \frac{10}{74} = 0.135$

Dilution factor, $D(W) = 1 - \frac{s.N_{carbon}(W)}{N_{C_4H_9OH}(W)}$

s : phase space scale factor - depends on kinematic variables

Photon energy correction

- $\Delta E = \sum E_i - 0.938 - E_{Photon}(mea)$
- E_i : E of the final state particles returned by kinematic fitter, $E_{Photon}(mea)$: from the Tagger

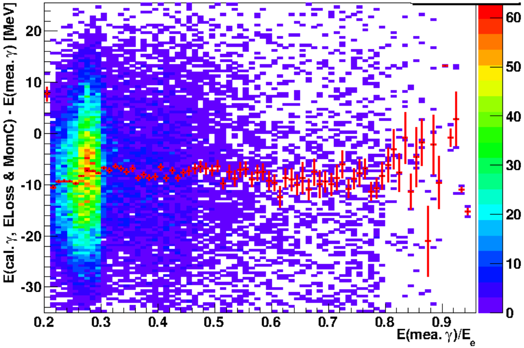

Photon energy correction

- Photon energy needs correction mainly because of sagging of the Tagger.
- Used the Photon E correction constructed by S. Park (a former FSU grad student) for his g9a analysis.